Current Research in Toxicology 7 (2024) 100194

Contents lists available at ScienceDirect

Current Research in Toxicology

journal homepage: www.journals.elsevier.com/current-research-in-toxicology

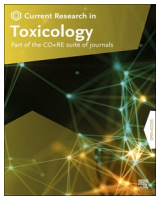

Research Paper

Cytotoxicity and inhibitory potential of CUDC-101 in non-small cell lung cancer cells with rare EGFR L861Q mutation

Chunhong Chu [a,b,1], Huixia Xu [a,1], Chenxue Liu [a], Xiangkai Wei [a], Lanxin Li [a], Rui Wang [a], Wenrui Cui [a], Guoliang Zhang [a,b], Chenyang Liu [a], Ke Wang [a], Lei An [a,b,*], Fei He [a,*]

[a] Translational Medicine Center, Huaihe Hospital of Henan University, Henan University, Kaifeng 475000, China
[b] Institutes of Traditional Chinese Medicine, School of Pharmacy, Henan University, Kaifeng 475000, Henan, China

ARTICLE INFO

Keywords:
L861Q
CUDC-101
Mutation
Proliferation
Cytotoxicology

ABSTRACT

The epidermal growth factor receptor (EGFR) represents an effective target for the treatment of non-small cell lung cancer. In the treatment of classical EGFR mutations, EGFR tyrosine kinase inhibitors have achieved desirable clinical efficacy. However, the effectiveness of tyrosine kinase inhibitors (TKIs) against the L861Q mutation has not been fully established. In this study, the four cell lines containing the L861Q mutation were constructed by CRISPR and the anti-tumour effects of CUDC-101 on them were investigated in vitro by various chemosensitivity methods, with afatinib serving as a positive control. The results demonstrated that CUDC-101 inhibited the proliferation and clonogenic capacity on the four cells through the ERK or AKT pathways, decreased the mitochondrial membrane potential of the cells, blocked the cell cycle and promoted apoptosis. Our findings suggest that CUDC-101 may be a promising treatment option for NSCLC patients with the EGFR exon 18 substitution mutation L861Q.

1. Introduction

Lung cancer is one of the most prevalent forms of cancer and the leading cause of cancer-related mortality worldwide. Global cancer statistics indicate that over two million individuals are diagnosed with lung cancer each year (Sung et al., 2021). From a pathological perspective, lung cancer is typically classified into two primary categories: small cell lung cancer (SCLC) and non-small cell lung cancer (NSCLC). The latter category encompasses the most prevalent histological subtypes, including adenocarcinoma, squamous cell carcinoma and large cell carcinoma (Zappa and Mousa, 2016). Non-small cell lung cancer (NSCLC) accounts for approximately 85 % of all new lung cancer cases, with small cell lung cancer accounting for the remaining 15 % (Gridelli et al., 2015). The discovery of epidermal growth factor receptor (EGFR) activating mutations in patients with lung adenocarcinoma has led to the development of a new family of biologics, tyrosine kinase inhibitors (TKIs), which have been shown to be effective in the treatment of these patients (Paliogiannis et al., 2015). These agents have transformed the clinical management of patients with EGFR mutations, nearly doubling survival and improving health-related quality of life compared to standard chemotherapy. In addition to EGFR, other common genetic alterations include ALK, KRAS, ROS1, BRAF, RET and HER-2 (An et al., 2023). These genetic mutations result in the abnormal proliferation and differentiation of cells, leading to the formation of a highly invasive and drug-resistant tumour (Lynch et al., 2004).

The two types of mutations, EGFR 19del and L858R, are designated as “classical” or “common” EGFR mutations, accounting for approximately 90 % of NSCLC mutations. It is postulated that these mutations induce comparable conformational alterations within the ATP-binding cleft of the protein (Bae et al., 2007). The remaining patients with EGFR mutations carry “rare” mutations, which account for 10–20 % of all EGFR mutations (Evans et al., 2019). L861Q is one of the less common mutations, which may be present in combination with other mutations, and accounts for approximately 1–2 % of EGFR mutations (Otsuka et al., 2015). A number of preclinical trials have demonstrated low efficacy or complete resistance to EGFR TKIs in the presence of the L861Q mutation (Furuyama et al., 2013; Kancha et al., 2011). However, it has recently been reported that with a reduction in dosage, afatinib can be used as a first-line therapy for patients with tumours carrying rare mutations (Kim et al., 2019). Afatinib is currently approved for the first-

* Corresponding authors at: No.115, Ximen Avenue, Huaihe Hospital of Henan University, Henan University, Kaifeng 475000, China.
E-mail addresses: anlei@henu.edu.cn (L. An), dr_feihe@henu.edu.cn (F. He).
[1] These authors contributed equally to this work.

https://doi.org/10.1016/j.crtox.2024.100194
Received 8 June 2024; Received in revised form 11 September 2024; Accepted 13 September 2024
Available online 22 September 2024

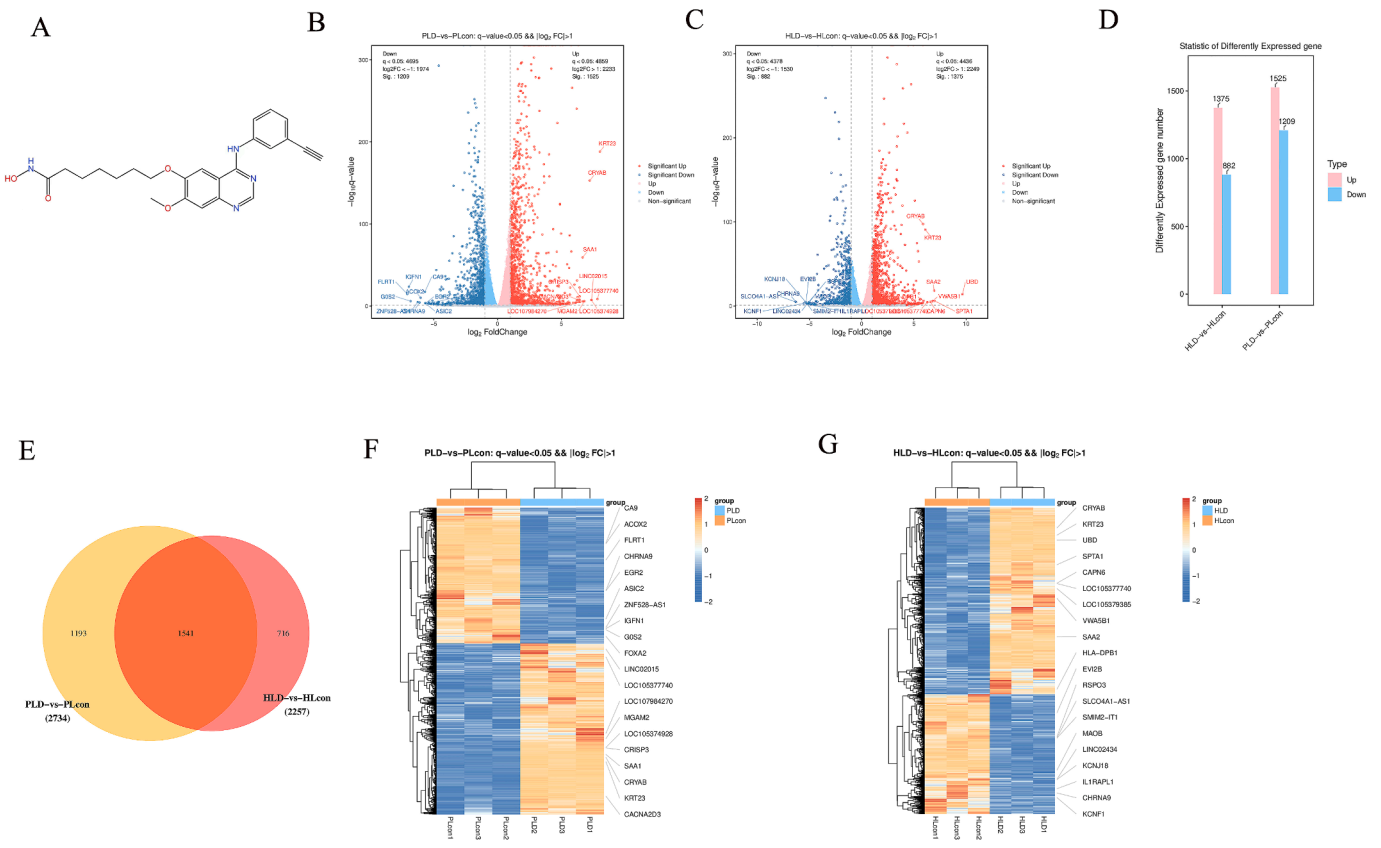

Fig. 1. The chemical structure of CUDC-101 and its effect on gene expression. (A) Chemical structural formula of compound CUDC-101; (B) and (C) show differentially expressed volcano plots; (D) Histogram of the statistics of differentially expressed genes of H3255$^{L861Q+L858R}$ and PC-9$^{L861Q+19del}$ treated with CUDC-101; (E) Statistical plots of the number of differentially expressed genes shared and unique to H3255$^{L861Q+L858R}$ and PC-9$^{L861Q+19del}$, respectively. (F) and (G) present a clustering diagram of differential gene grouping.

line treatment of metastatic non-small cell lung cancer (NSCLC) carrying non-resistant EGFR point mutations (S768I, L861Q, G719X) and classical EGFR mutations (Wu et al., 2014).

The efficacy of EGFR inhibitors is limited due to primary and acquired resistance to EGFR inhibitors. Recently, combining histone deacetylase (HDAC) inhibitors with chemotherapeutic drugs, especially EGFR inhibitors, has been considered as one of the most encouraging strategies to enhance the efficacy of antineoplastic drugs and reduce or avoid drug resistance (Ibrahim et al., 2021). CUDC-101 has been identified as a multi-target inhibitor (Fig. 1A), which simultaneously blocks HDACs, EGFR and human epidermal growth factor 2 receptor. This has been demonstrated to have anti-tumour activity in several thyroid and pancreatic cancer cell lines (Ji et al., 2018; Zhang et al., 2015).

In order to investigate the sensitivity of the EGFR L861Q mutation to CUDC-101, four cell lines were constructed containing the EGFR L861Q mutation. These were created by gene editing method and are designated as follows: H3255^{L861Q}, H3255$^{L861Q+L858R}$, PC9^{L861Q} and PC9$^{L861Q+19del}$. The experiments aimed to verify the inhibition of AKT and ERK phosphorylation in a dose-dependent manner, as well as the inhibition of apoptosis and cell proliferation, which may offer novel avenues for drug discovery and clinical precision.

2. Materials and methods

2.1. Drugs and reagents

CUDC-101 was purchased from Shanghai Selleck Chemicals (China). The HEK-293T, H3255, and PC-9 cell lines were obtained from the laboratory deposit. All molecular cloning reagents were procured from New England Biolabs (NEB, USA). RPMI-1640 medium, DMEM medium, foetal bovine serum (FBS), phosphate-buffered saline (PBS), trypsin, penicillin and streptomycin were sourced from Gibco (Carlsbad, USA). Puromycin and blasticidin S HCl (BSD) were procured from Thermo Fisher Scientific (USA). 3-(4,5-dimethylthiazol-2-yl)-2,5-diphenyl-2H-tetrazolium bromide (MTT), protease inhibitor and phosphatase inhibitor were obtained from Beijing Sola Biotechnology Co., Ltd (China). The EdU Cell Proliferation Kit with Alexa Fluor 555, Mitochondrial Membrane Potential and Apoptosis Detection Kit with Mito-Tracker Red CMXRos Annexin V-FITC, PI were purchased from Beyotime Biotechnology (China). The EGFR, pEGFR, AKT, pAKT, ERK, pERK, GAPDH and HRP-labelled secondary anti-mouse/anti-rabbit antibodies were obtained from ProteinTech Co., Ltd (China).

2.2. Cell culture

The DMEM medium was used for HEK 293T cells containing 10 % fetal bovine serum (FBS, Clark Bioscience, China), 100 U/ml penicillin and 100 μg/ml streptomycin. The H3255-Cas9 and PC-9-Cas9 cells were cultured in RPMI 1640 medium, which was supplemented with 10 % fetal bovine serum, 100 U/ml penicillin, 100 μg/ml streptomycin, and 2 μg/ml puromycin hydrochloride (Puromycin; Thermo Fisher Technologies, Waltham, MA, USA). All cell lines were maintained in an incubator at 37 °C with 5 % CO_2. The cells were treated with 0.2 μM, 0.4 μM, 0.8 μM and 1.6 μM CUDC-101 at a drug concentration for 48 h, and were subsequently used for further experiments.

2.3. Cell lines establishment for H3255$^{L861Q+L858R}$ and PC-9$^{L861Q+19del}$ mutant

The HEK-293T (A Human renal epithelial cell line), The H3255 (A

Table 1
The kinase inhibitory activity of CUDC-101 against EGFR mutations (IC_{50}, nmol/L).

Cell line	IC_{50}	Cell line	IC_{50}
H3255	232.7 nM	PC-9	210.3 nM
$H3255^{L861Q+L858R}$	484.5 nM	$PC\text{-}9^{L861Q+19del}$	580.0 nM
$H3255^{L861Q}$	607.4 nM	$PC\text{-}9^{L861Q}$	373.3 nM

Human lung cell line with EGFR L858R mutant), and PC-9 cell lines (A Human lung adenocarcinoma cell line with EGFR 19 exon deletion mutant) was used in this study. Based on this background, two groups of human lung cancer cell lines H3255 (background EGFR L858R mutation) and PC-9 (background EGFR 19del mutation) with mutation EGFR L861Q were selected as the basis for modification. Briefly, we transduced EGFR L861Q, psPAX2 and pMD2G into HEK293 cells thereby generating lentiviruses containing EGFR L861Q, which were then cultured in H3255 and PC-9 cells and screened for 14 days of passaging culture using medium containing 10 μg/mL BSD thereby constructing NCI- $H3255^{L861Q+L858R}$ and NCI-$PC\text{-}9^{L861Q+19del}$ cell lines were constructed. This protocol were conducted as previous study (Liu et al., 2022; Wang et al., 2023a).

2.4. Cell lines establishment for $H3255^{L861Q}$ and $PC\text{-}9^{L861Q}$ mutant

The PLenti-EF1α-Cas9 plasmid was packaged as previously described (Liu et al., 2022), and then the lentiviral fragment PLenti-EF1α-Cas9 plasmid was infected into H3255 cells and PC-9 cells, respectively. Following 14 days of BSD screening, the H3255-Cas9 cell line and PC-9-Cas9 cell line were established. Lentiviral particles containing the pLenti-EGFR-L861Q plasmid (previously packaged in 2.3) were then infected with H3255-Cas9 cells and PC-9-Cas9 cells, respectively. Following a 14-day screening period with BSD and puromycin, the $PC\text{-}9^{L861Q}$ cell line and the $H3255^{L861Q}$ cell line were successfully established. The cells were then cultured in 1640 medium containing 10 μg/mL BSD and 2 μg/mL puromycin.

2.5. Transcriptome sequencing

The $PC\text{-}9^{L861Q+19del}$ and $H3255^{L861Q+L858R}$ cells in the logarithmic growth phase were taken and inoculated in 10 cm dishes at a density of 2.5 million cells per well. The cells were incubated overnight in an incubator and medium was replaced by fresh with prepared CUDC-101 at a concentration of 0.4 μM was added. After 48 h, the incubation was terminated and RNA was extracted using Trizol. The extracted RNA was

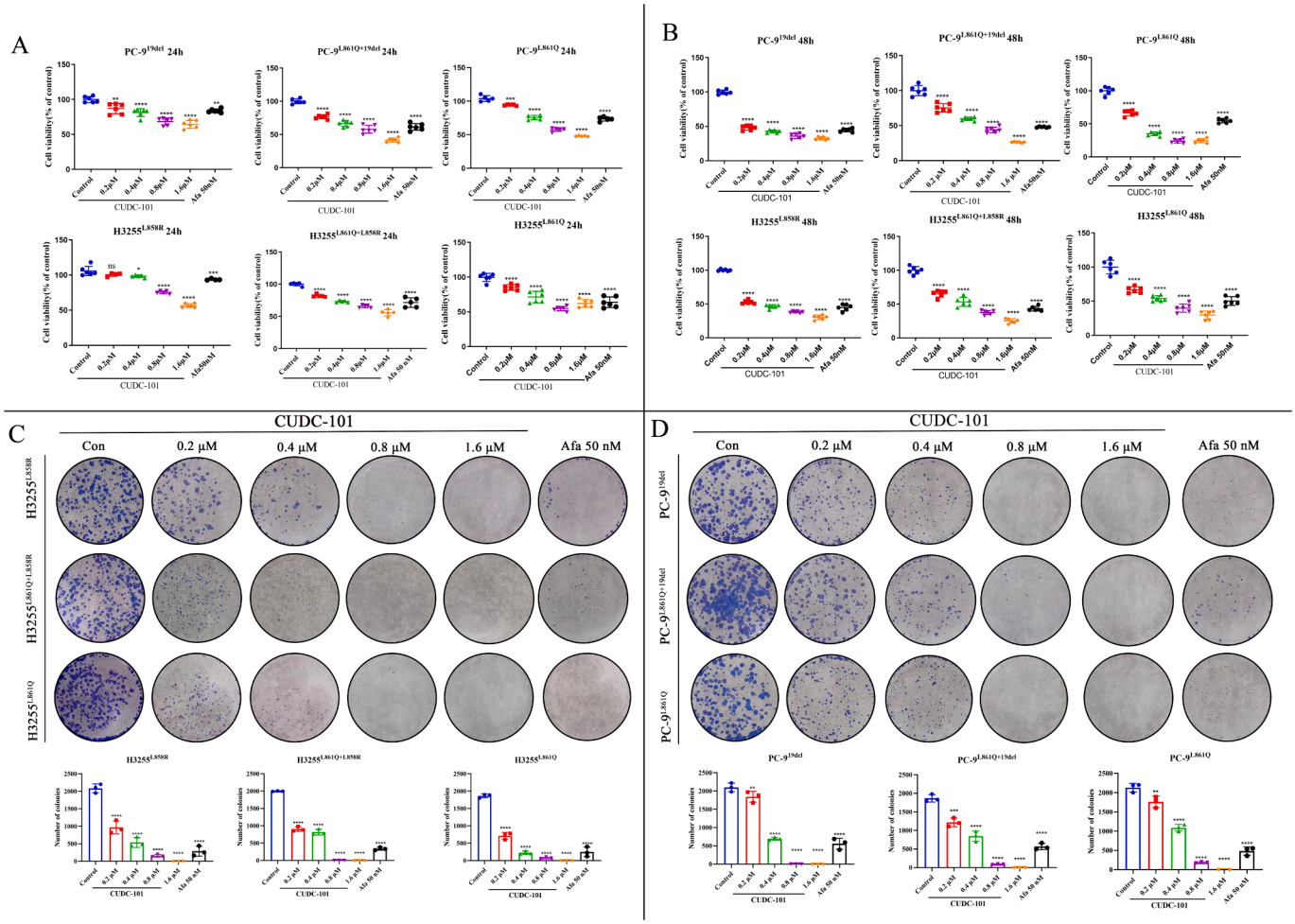

Fig. 2. The effect of CUDC-101 on cell viability. (A) The cell viability of PC-9, $PC\text{-}9^{L861Q+19del}$, $PC\text{-}9^{L861Q}$, H3255, $H3255^{L861Q+L858R}$ and $H3255^{L861Q}$ was determined 24 h after the addition of CUDC-101 or afatinib; (B) 48 h after the addition of CUDC-101 or afatinib, the cell viability of six groups of cells was determined. (C) H3255, $H3255^{L861Q+L858R}$ and $H3255^{L861Q}$ were treated with CUDC-101 or afatinib and then allowed to form colonies for 14 days. The cells were fixed and stained with crystal violet, and the colonies were quantified. (D) The PC-9, $PC\text{-}9^{L861Q}$ and $PC\text{-}9^{L861Q+19del}$ cell lines were treated and then allowed to form colonies for 14 days. The cells were fixed and stained with crystal violet, and the colonies were quantified. The data are expressed as a one-way ANOVA for three independent experiments. The results were not statistically significant (ns), or significant at the 0.05, 0.01, 0.001, and 0.0001. (For interpretation of the references to colour in this figure legend, the reader is referred to the web version of this article.)

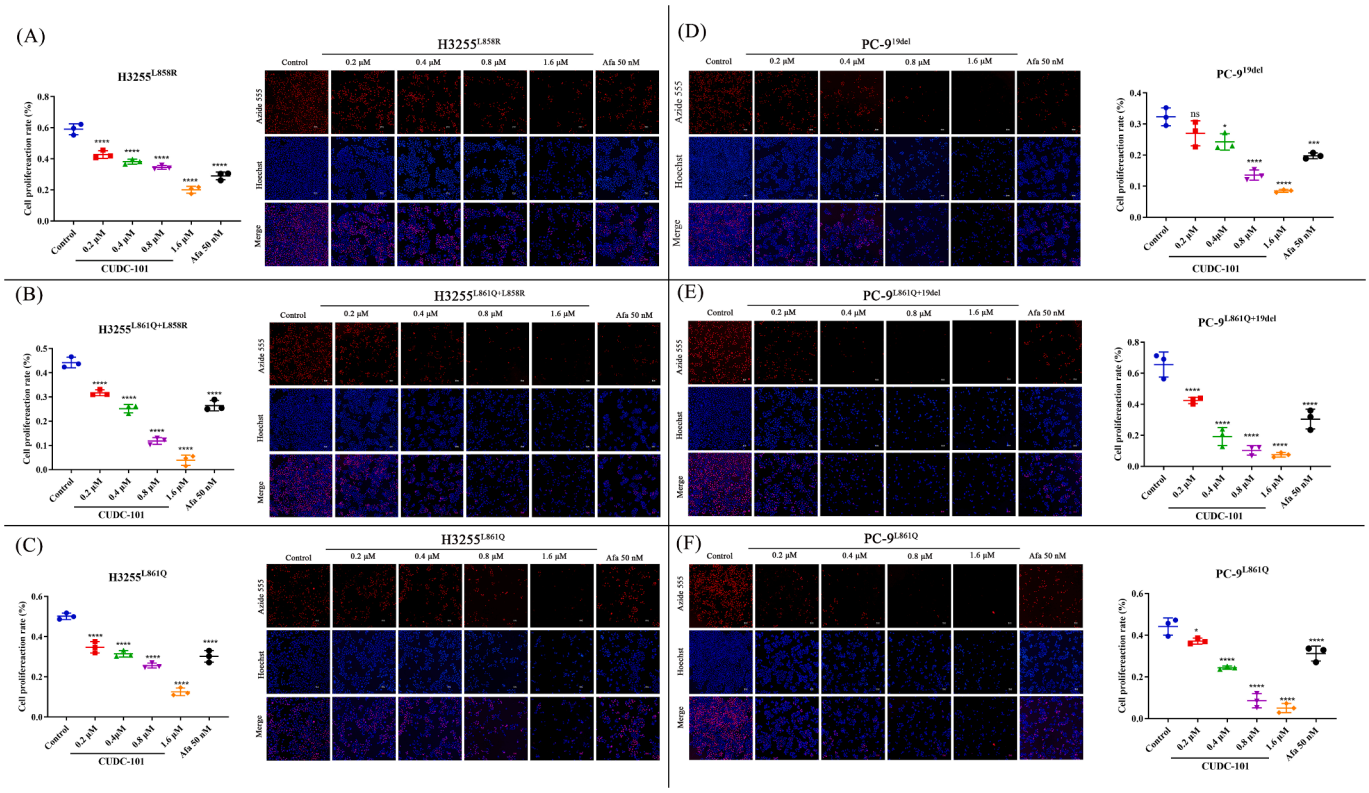

Fig. 3. The effect of CUDC-101 on cell proliferation. (A) The cell proliferation results for the H3255 cell line; (B) The cell proliferation results for the H3255$^{L861Q+L858R}$ cell line; (C) The cell proliferation results for the H3255^{L861Q} cell line; (D) The cell proliferation results for the PC-9 cell line; (E) The cell proliferation results for the PC-9$^{L861Q+19del}$ cell line; (F) The cell proliferation results for the PC-9^{L861Q} cell line. Proliferating cells were labelled with Azide 555 while the nuclei of all cells were labelled with Hoechst 33342 at 100× original magnification. Scale bar, 50 μm. The data are expressed as mean ± SD of three independent experiments. Statistical significance was observed at $^{*}p < 0.05$, $^{**}p < 0.01$, $^{***}p < 0.001$ and $^{****}p < 0.0001$, when compared to the control.

stored on dry ice and three independent replicates were conducted for each sample. Transcriptome sequencing was performed using the Oebiotechnology sequencing platform. The raw data was optimised for high-quality clean reads. The counts of individual sample genes were normalised using the DESeq2 software. The fold change (FC) indicates the expression rate between two groups of samples, with a screening criterion of Log2 FC > 2, $p \leq 0.05$. Multiple tests were performed to statistically determine significant differences, which were corrected for false discovery rate (FDR). The objective of the differential expression analysis was to identify genes that exhibited differential expression between the different samples. The differentially expressed genes were enriched in the Gene Ontology (GO) and Kyoto Encyclopedia of Genes and Genomes (KEGG) databases.

2.6. Cell survival assay

Cell survival and viability were assessed using the MTT assay. The H3255, H3255^{L861Q}, H3255$^{L861Q+L858R}$, PC-9, PC-9^{L861Q} and PC-9$^{L861Q+19del}$ cells in logarithmic growth phase were inoculated into 96-well plates at a density of 5000 cells per well. The outer ring of the 96 wells plate was filled with phosphate-buffered saline (PBS) and incubated overnight at 37 °C with 5 % CO_2, the medium was removed from each well and replaced with CUDC-101 or afatinib for 24 and 48 h. After that, 5 mg/mL MTT was added to each well and incubated at 37 °C for 4 h. Finally, the supernatant was discarded, and 100 μl of DMSO (Dimethyl sulfoxide) solution was added to each well. Optical density (OD) was measured using a microplate reader to determine cell viability at 490 nm.

2.7. Colony formation assay

Upon reaching 85 % cell abundance, the cells of H3255, H3255^{L861Q}, H3255$^{L861Q+L858R}$, PC-9, PC-9^{L861Q} and PC-9$^{L861Q+19del}$ were digested and counted. A cell suspension of 250 cells/mL was prepared, and the plates were spread at a density of 500 cells/well. Subsequently, the cell culture medium was aspirated after 18 h, and the cells were maintained in a fresh medium containing the drug solution for a further 12–14 days. RPMI-1640 complete medium was added to the control group, while the drug-dosing group was added with 0.2 μM、0.4 μM、0.8 μM、1.6 μM CUDC-101 and 50 nM afatinib. Once the clones had become visible to the naked eye at the bottom of the 6-well plate, the plate was removed from the incubator, the medium was aspirated, and then fixed in 4 % paraformaldehyde for 20 min. Subsequently, the clonogenic capacity of the cells was determined by dividing the number of colonies in the drug-treated group by the number of colonies in the control group.

2.8. EdU cell proliferation assay

The 5-Ethyl-2′-deoxyuridine (EdU) assay was conducted in three wells using commercially available kits in accordance with the instructions. In brief, the EdU solution was diluted with medium and added to the cells incubated for 2 h at 37 °C. Following two washes with 1 × PBS, the cells were fixed with 4 % paraformaldehyde and treated with 0.3 % Triton X-100 in PBS. Subsequently, the cells were incubated with 50 μL of the prepared Click Additive Solution (43 μL Click Reaction Buffer、2 μL CuSO4、0.1 μL Azide 555 and 4.9 μL Click Additive Solution). The nuclei were then stained with 50 μL of 1 × Hoechst 33342. The cells were imaged using fluorescence microscopy. The cell proliferation rate was calculated using Image J software, and the cells were counted.

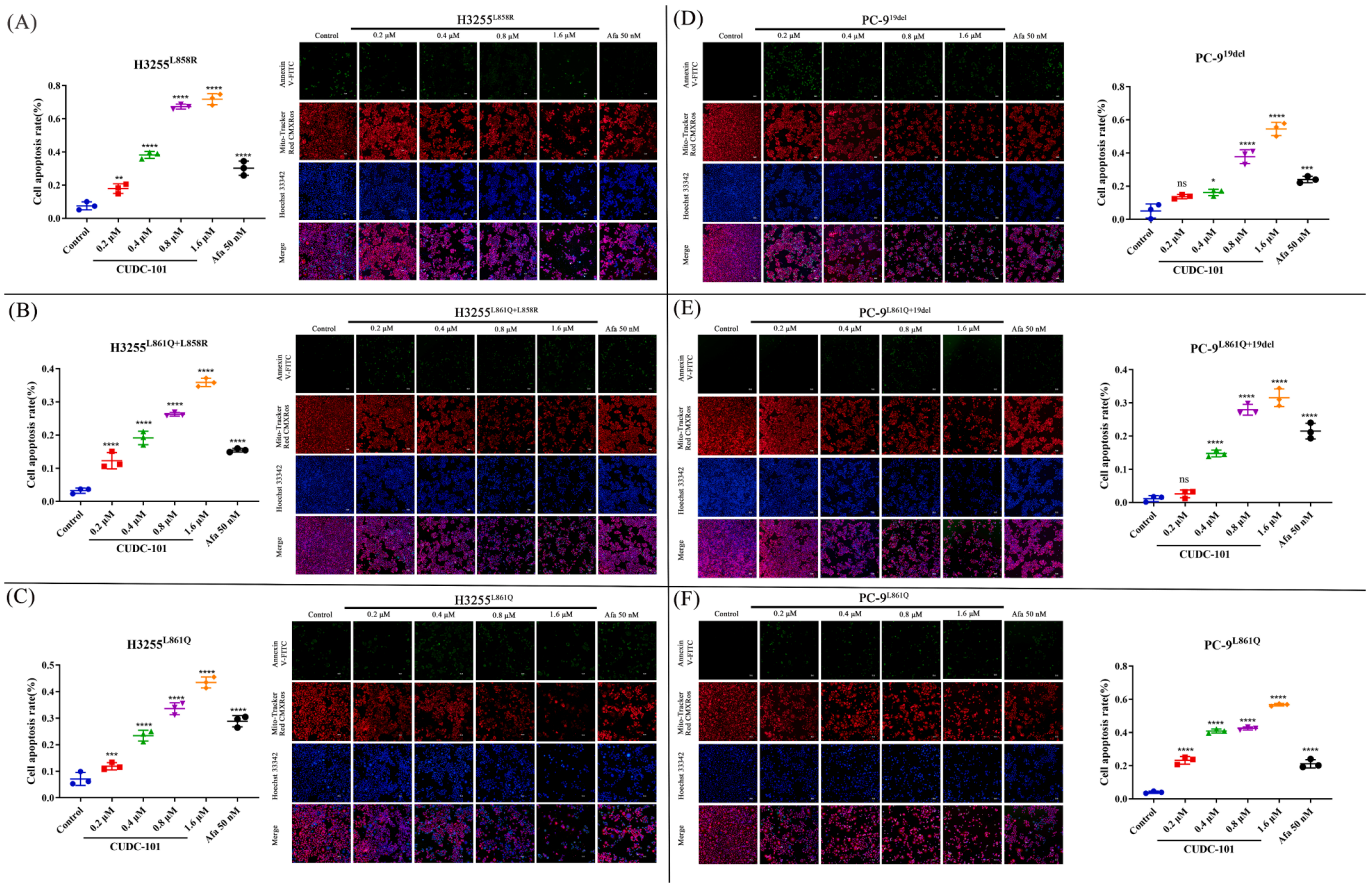

Fig. 4. Fluorescence detection was used to measure mitochondrial membrane potential and apoptosis in H3255 and PC9 cells treated with CUDC-101. (A) The mitochondrial membrane potential results is observed in the H3255 cell line; (B) The mitochondrial membrane potential results is observed in the $H3255^{L861Q+L858R}$ cell line; (C) The mitochondrial membrane potential results is observed in the $H3255^{L861Q}$ cell line. (D) The mitochondrial membrane potential results is observed in the PC-9 cell line; (E) The mitochondrial membrane potential results is observed in the $PC\text{-}9^{L861Q+19del}$ cell line; (F) The mitochondrial membrane potential results is observed in the $PC\text{-}9^{L861Q}$ cell line; (G) The results represent the apoptosis in the six cell lines. The red fluorescence indicates the mitochondrial membrane potential, the blue fluorescence indicates all nuclei, and the green fluorescence indicates apoptotic cells. Scale bar, 50 μm. The data are expressed as mean ± SD of three independent experiments. The results were not statistically significant when compared with the control group (ns). The following symbols were used to indicate the level of significance, *$p < 0.05$, **$p < 0.01$, ***$p < 0.001$, ****$p < 0.0001$. (For interpretation of the references to colour in this figure legend, the reader is referred to the web version of this article.)

2.9. Mitochondrial membrane potential assay and apoptosis

The cells were centrifuged at 1000 g for 5 min following the Mitochondrial Membrane Potential and Apoptosis Detection Kit (Mito-Tracker Red CMXRos, Beyotime, China). The cell culture medium was removed, and the cells were washed with 100 μl of PBS per well. The solutions were mixed gently. Then, 32 μL of Annexin V-FITC conjugate and 0.34 μL of Mito-Tracker Red CMXRos staining solution were added to each well, followed by 0.84 μL of Annexin V-FITC and 0.84 μL of Hoechst staining solution for 30 min at room temperature. Then, placed the sample in an ice bath and observed it immediately under a fluorescence microscope (Nikon Ti2-E, Japan).

2.10. Detection of apoptosis by flow cytometry

The 6×10^5 cells were used with CUDC-101 and afatinib at a concentration for flow cytometry. In brief, the cells were washed with PBS, digested, and collected by centrifugation at 1000 x g for 5 min. The cells were washed again with PBS and resuspended. The apoptosis rate was determined by flow cytometry after labelling apoptotic cells with the 5 μL PI and Annexin V-FITC (Apoptosis Detection Kit, Procell, China) for 15 min. The percentages of Annexin V-positive cells in the apoptosis plots were added and analysed.

2.11. Western blot analysis

The cells were resuspended in PBS and collected at 4 °C, for 5 min. A mixture of protease and phosphatase inhibitors was added to the RIPA lysis buffer, and the concentration was subsequently quantified using a BCA protein assay kit. All samples were added to a 10 % SDS-PAGE gel of the same volume and the gel was transferred to an NC membrane (Pall Corporation, USA), which was closed in 5 % skimmed milk for 1 h at room temperature. Subsequently, the primary antibodies were added at the indicated dilutions and incubated overnight at 4 °C. The membrane was washed three times for five minutes each time using phosphate-buffered saline (PBS) containing 0.1 % Tween 80 (PBST) and then incubated with secondary antibodies. The following antibodies were used: anti-EGFR (1:1000), anti-p-EGFR (1:1000), anti-ERK (1:5000), anti-p-ERK (1:5000), anti-Akt (1: 1000), anti-p-Akt (1:2000), anti-HO-1 (1:5000), anti-GAPDH (1:5000), anti-rabbit IgG (1:5000), and anti-GAPDH (1:5000).

2.12. Statistical analysis

All data are expressed as mean ± SEM, and data were statistically analyzed between groups using one-way ANOVA of three independent experiments. Drawn with GraphPad Prism 8.0 software. The results showed statistical significance with *$p < 0.05$, **$p < 0.01$, ***$p < 0.001$,

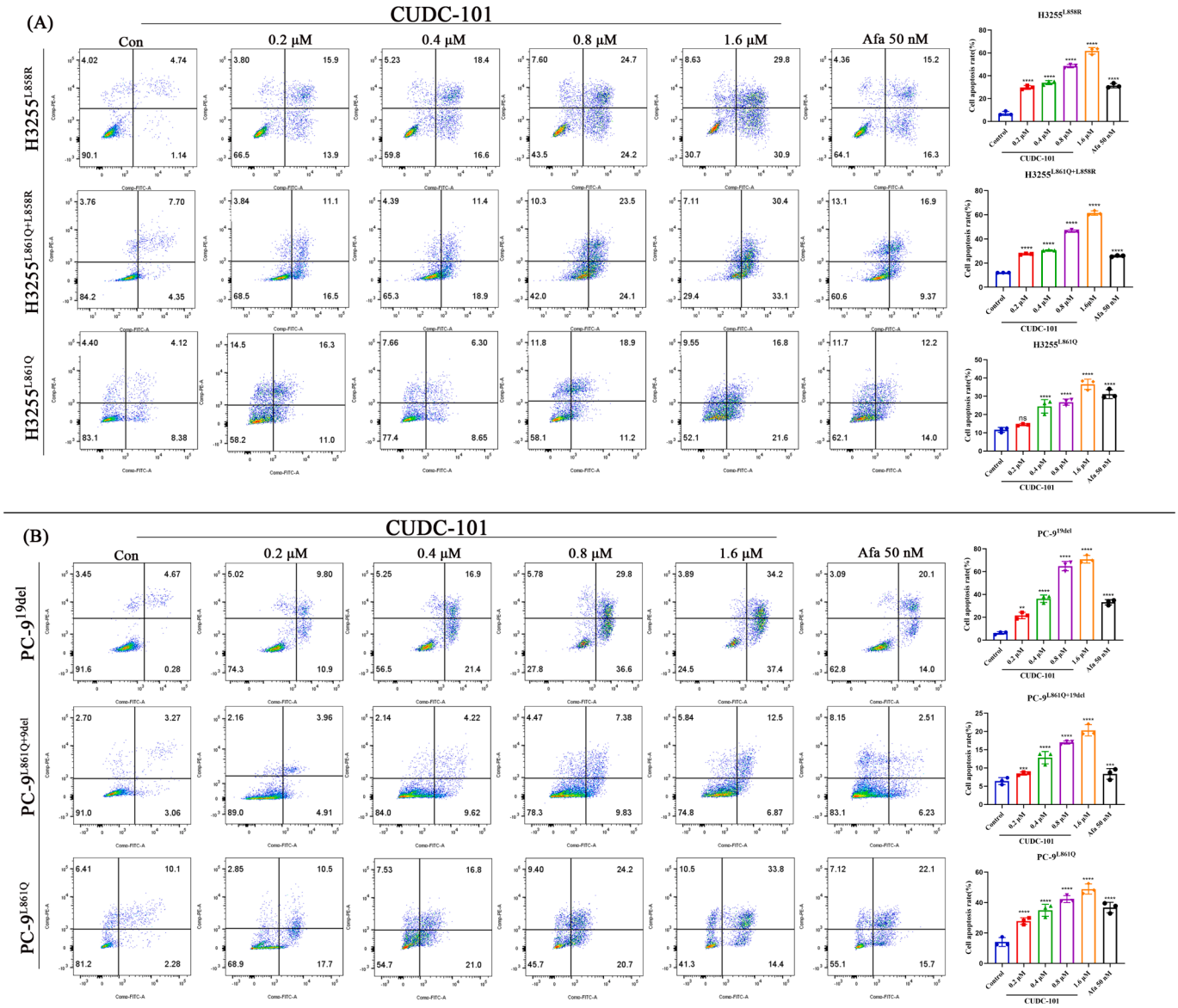

Fig. 5. CUDC-101 induces apoptosis of EGFR L861Q cell lines. The apoptosis level of the cells was determined by flow cytometry. (A) H3255, H3255$^{L861Q+L858R}$ and H3255^{L861Q} were treated with CUDC-101 or afatinib for 48 h. (B) PC-9, PC-9$^{L861Q+19del}$ and PC-9^{L861Q} were treated with CUDC-101 or afatinib for 48 h. The apoptotic rates of the six groups treated with CUDC-101 or afatinib were analysed in the Q2 and Q3 phases. The data are expressed as a one-way ANOVA for three independent experiments. The results were either non-significant (ns) or significant at *$p < 0.05$, **$p < 0.01$, ***$p < 0.001$ and ****$p < 0.0001$.

****$p < 0.0001$.

3. Results

3.1. Transcriptome sequencing analysis

The results of the analysis demonstrated that the percentage of effective bases, Q30 and GC content of all samples met the requisite standards for subsequent analysis (Supplementary Table 1). Some genes exhibited differential expression following treatment of cells with CUDC-101, as evidenced by the histogram of differentially expressed genes (Fig. 1D) that in the H3255$^{L861Q+L858R}$ cell line, the total number of differentially expressed genes was 2257, with up-regulated 1375 genes and down-regulated 882 genes. In the PC-9$^{L861Q+19del}$ cell line, the total number of differentially expressed genes was 2734, with up-regulated 1525 genes and down-regulated 1209 genes. The results illustrate the shared and unique differentially expressed genes between the different comparison groups (Fig. 1E). The differentially expressed volcano plots (Fig. 1B and C) provide an overview of the overall distribution of differentially expressed genes.

In the H3255$^{L861Q+L858R}$ cell line, the expression of genes such as SLCO4A1-AS1, KCNF1, LINC02434 and EVI2B was significantly reduced ($p < 0.05$), while the expression levels of genes such as UBD, VWA5B1, SPTA1, SAA2, and CAPN6 were significantly increased ($p < 0.05$). In the PC-9$^{L861Q+19del}$ cell line, the expression levels of genes such as G0S2, FLRT1, IGFN1 and CA9 were significantly reduced ($p < 0.05$), while the expression levels of genes such as KRT23, CRYAB, SAA1, LINCO2015, and LOC105377740 were significantly increased ($p < 0.05$) following the CUDC-101 treatment. Our results also illustrate the cluster analysis diagram of differential gene grouping (Fig. 1F and G), and the horizontal axis represents the name of the sample, while the vertical axis displays all the differential genes (Top10 genes).

Unlike cells H3255$^{L861Q+L858R}$ treated with CUDC-101 (Supplementary Fig. 1A and B), the results indicated that, in PC-9$^{L861Q+19del}$ cells following treatment with CUDC-101, the up-regulated genes were an enrichment of subentries related to the immune response,

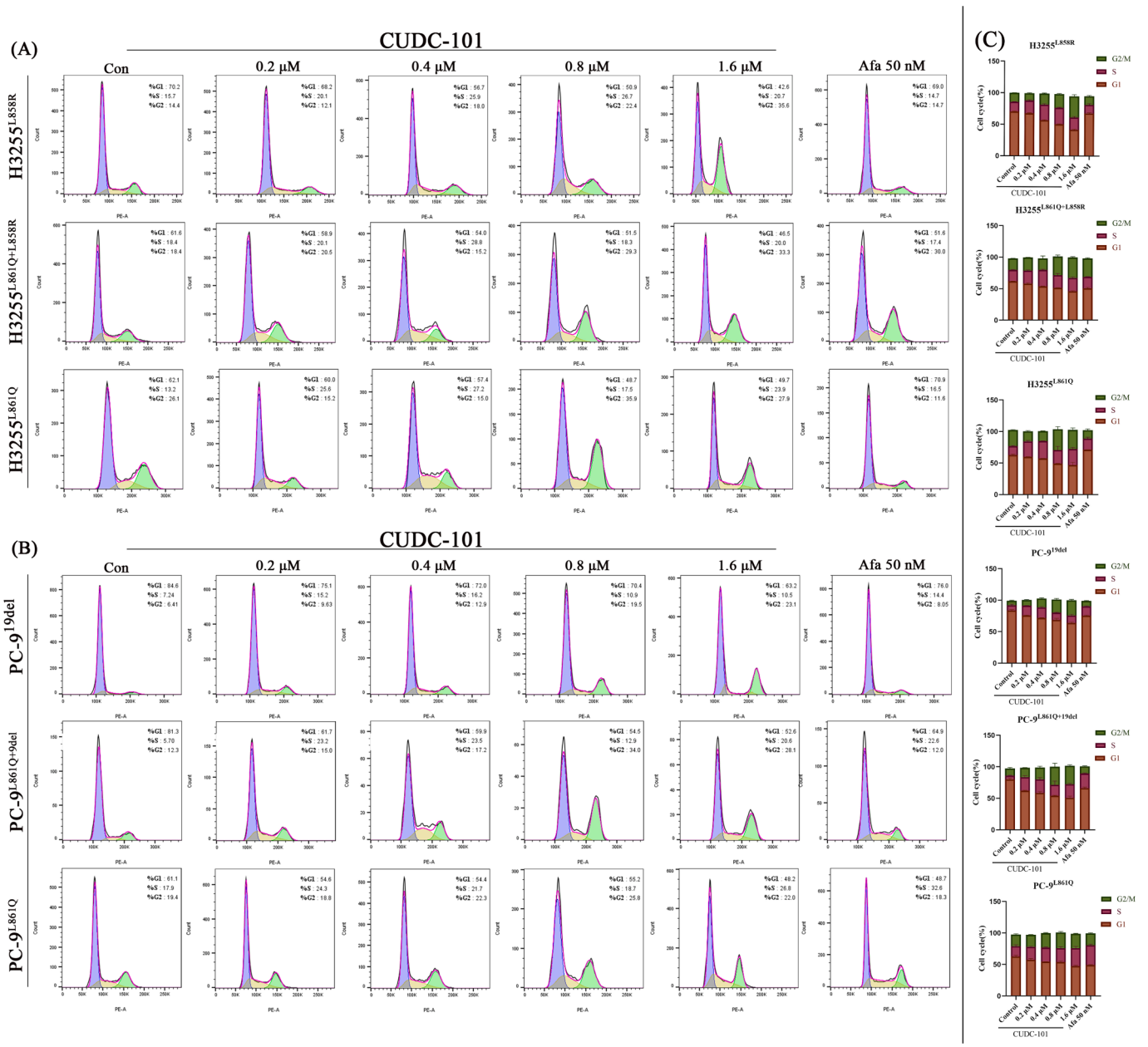

Fig. 6. Effect of CUDC-101 on cell cycle. (A) The cell cycle results for H3255, H3255$^{L861Q+L858R}$ and H3255^{L861Q}. (B) The cell cycle results for PC-9, PC-9$^{L861Q+19del}$ and PC-9^{L861Q}. The data were processed and analysed using Flow Jo 10.8.1 software. (C) The cell cycle analysis of CUDC-101 at G2/M, S and G1 with afatinib as control.

extracellular exosomes, the plasma membrane, calcium ion binding, and signalling receptor binding (Supplementary Fig. 1C). The down-regulated genes were an enrichment of subentries related to immune response, signalling receptor binding and calcium ion binding (Supplementary Fig. 1D), the subentries for mitotic sister chromatid segregation, cell division, kinetochore, centrosome, ATP binding and microtubule binding. A functional enrichment analysis of the differentially expressed genes screened in the control and experimental groups revealed that CUDC-101 activated the cellular immune response mechanism, inhibited the cellular ATP functional response, and blocked cell proliferation.

Unlike cells H3255$^{L861Q+L858R}$ treated with CUDC-101 (Supplementary Fig. 1E and F), the up-regulated genes on biological pathways in PC-9$^{L861Q+19del}$ cells following treatment with CUDC-101 (Supplementary Fig. 1G) were primarily enriched to the FoxO signalling pathway, the IL-17 signalling pathway, Staphylococcus aureus infection, and inflammatory bowel disease. These pathways were associated with apoptosis and immune responses. The down-regulated genes on biological pathways were mainly enriched to the cell cycle, Rap1 signalling pathway, DNA replication, and purine metabolism, which are related to cell metabolism and cell growth (Supplementary Fig. 1H). The results presents a comparative map of the distribution of differentially expressed genes (KEGG) after CUDC-101 treatment in H3255$^{L861Q+L858R}$ and PC-9$^{L861Q+19del}$ (Supplementary Fig. 2). The differential target genes corresponding to the differential transcription factors were presented in Supplementary Fig. 3, and the protein interaction network map was constructed by combining the annotation of differential genes and transcription factors (Supplementary Fig. 4).

3.2. *CUDC-101 inhibits cell viability, colony formation and proliferation*

To examine the impact of CUDC-101 on cell viability, a series of cell

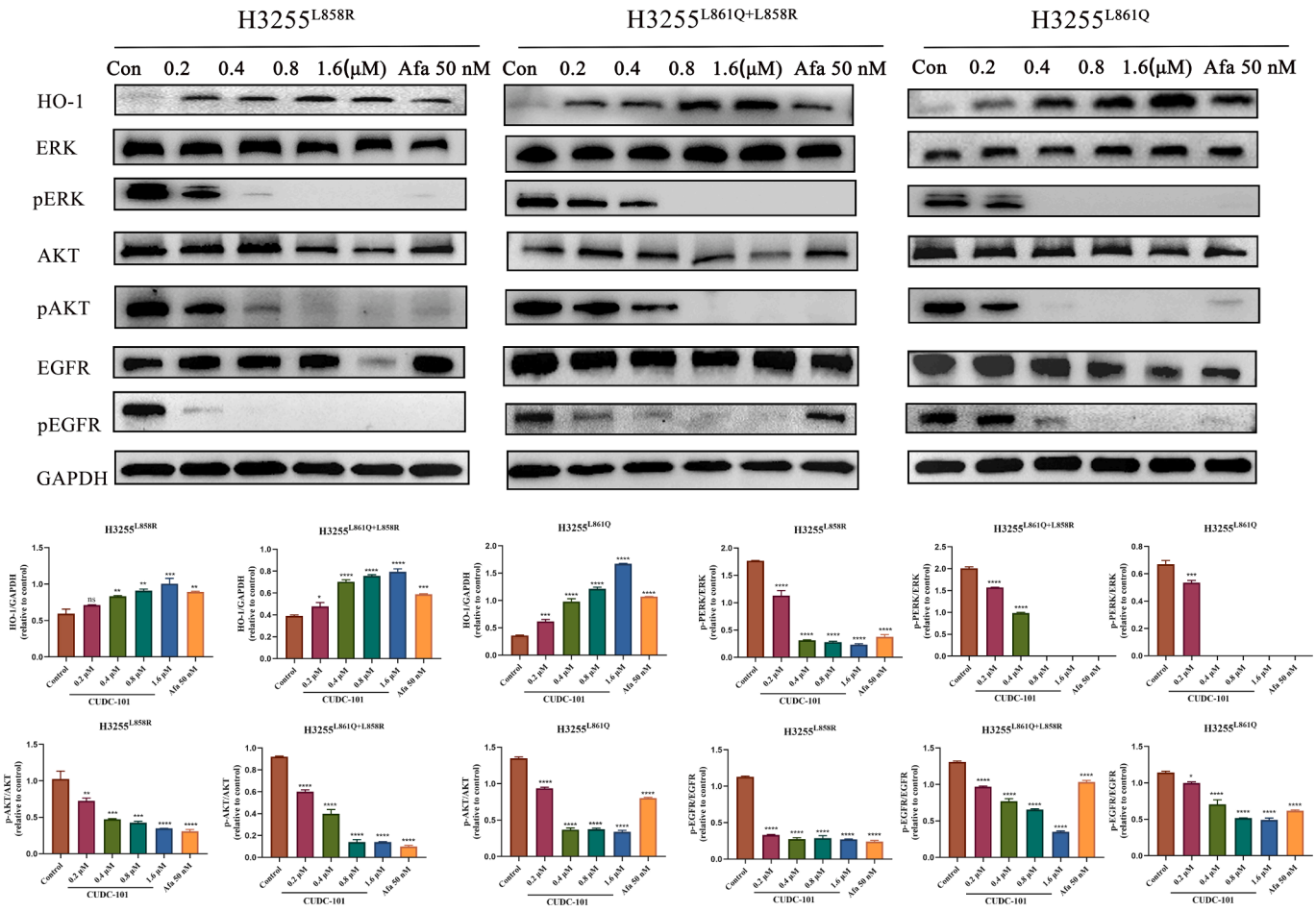

Fig. 7. Effects of CUDC-101 on the expression of relevant proteins in H3255 cell lines. (A) Western blot analysis of the activation of EGFR signalling as indicated by pEGFR, pAKT and pERK levels, and western blot analysis of HO-1 in the three groups cells, H3255, H3255$^{L861Q+L858R}$, and H3255^{L861Q} for 48 h with CUDC-101 or afatinib. The ratios of pEGFR/EGFR, pAKT/AKT, pERK/ERK and HO-1/GAPDH were quantified and analysed by Image J software. The data are expressed as a one-way ANOVA for three independent experiments. The results were not statistically significant (ns) or significant at the levels of $^{*}p < 0.05$, $^{**}p < 0.01$, $^{***}p < 0.001$ and $^{****}p < 0.0001$.

lines including H3255, H3255^{L861Q}, H3255$^{L861Q+L858R}$, PC-9, PC-9^{L861Q}, and PC-9$^{L861Q+19del}$ were treated for 24 and 48 h. The cell viability was then measured using the MTT assay after 48 h of incubation, CUDC-101 demonstrated potent and dose-dependent inhibition of H3255 cells (IC_{50} = 232.7 nmol/L), H3255$^{L861Q+L858R}$ cells (IC_{50} = 484.5 nmol/L), H3255^{L861Q} cells (IC_{50} = 607.4 nmol/L), PC-9 cells (IC_{50} = 210.3 nmol/L), PC-9$^{L861Q+19del}$ cells (IC_{50} = 580.0 nmol/L) and PC-9^{L861Q} cells (IC_{50} = 373.3 nmol/L) (Table 1). The results demonstrated that exposure to CUDC-101 resulted in a significant reduction in cell viability of the six cell lines in a dose- and time-dependent manner in comparison to the control group ($p < 0.0001$, Fig. 2A and B).

In order to assess the inhibitory effect of CUDC-101 on cell proliferation, colony formation assays were conducted with CUDC-101 (0.2 μM, 0.4 μM, 0.8 μM, 1.6 μM) and 50 nM Afatinib after 48 h of treatment. The results demonstrated that the colony formation capacity in H3255, H3255^{L861Q}, H3255$^{L861Q+L858R}$, PC-9, PC-9^{L861Q}, and PC-9$^{L861Q+19del}$ was significantly suppressed (Fig. 2C and D) following CUDC-101 treatment, resulting in a notable decline in the colony formation rate ($p < 0.0001$), indicating that treatment with CUDC-101 results in a reduction in the clonogenic ability in these cells.

Furthermore, the proliferative capacity in these six cells was determined using the EdU method (Cell Proliferation Assay Kit). The results demonstrated that the proliferation capacity in the six cells was significantly diminished following treatment with CUDC-101 and Afatinib in comparison to the control group (Fig. 3). It is noteworthy that the inhibitory effects on H3255^{L861Q}, H3255$^{L861Q+\ L858R}$, PC-9 and PC-9^{L861Q} at a concentration of 0.4 μM CUDC-101 were comparable to those of 50 nM Afatinib. In PC-9$^{L861Q+19del}$ cells, CUDC-101 at 0.2 μM demonstrated a pronounced inhibitory effect, accompanied by a relatively weaker inhibition of proliferation in H3255 cells.

3.3. CUDC-101 promotes apoptosis while decreasing mitochondrial membrane potential

A further examination of the mitochondrial membrane potential was conducted using the Mitochondrial Membrane Potential and Apoptosis Detection Kit. The number of cells was quantified using the Image J software and the apoptosis rate was plotted and analysed (Fig. 4). In comparison to the control group, the apoptotic percentage of H3255, H3255^{L861Q}, H3255$^{L861Q+L858R}$, PC-9, PC-9^{L861Q} and PC-9$^{L861Q+19del}$ was found to have significantly increased following treatment with CUDC-101 (0.2 μM, 0.4 μM, 0.8 μM, and 1.6 μM). The results demonstrated that CUDC-101 induced the mitochondrial apoptotic pathway in six NSCLC cells.

To assess the effect of CUDC-101-induced apoptosis, the apoptosis rates of CUDC-101-treated and control groups were compared using Annexin V/PI double staining. The six group cells were treated with CUDC-101 (0.2 μM, 0.4 μM, 0.8 μM, 1.6 μM) and 50 nM afatinib for 48 h, and the results were analysed using flow cytometry. The results demonstrated that CUDC-101 induced cell death in a concentration-

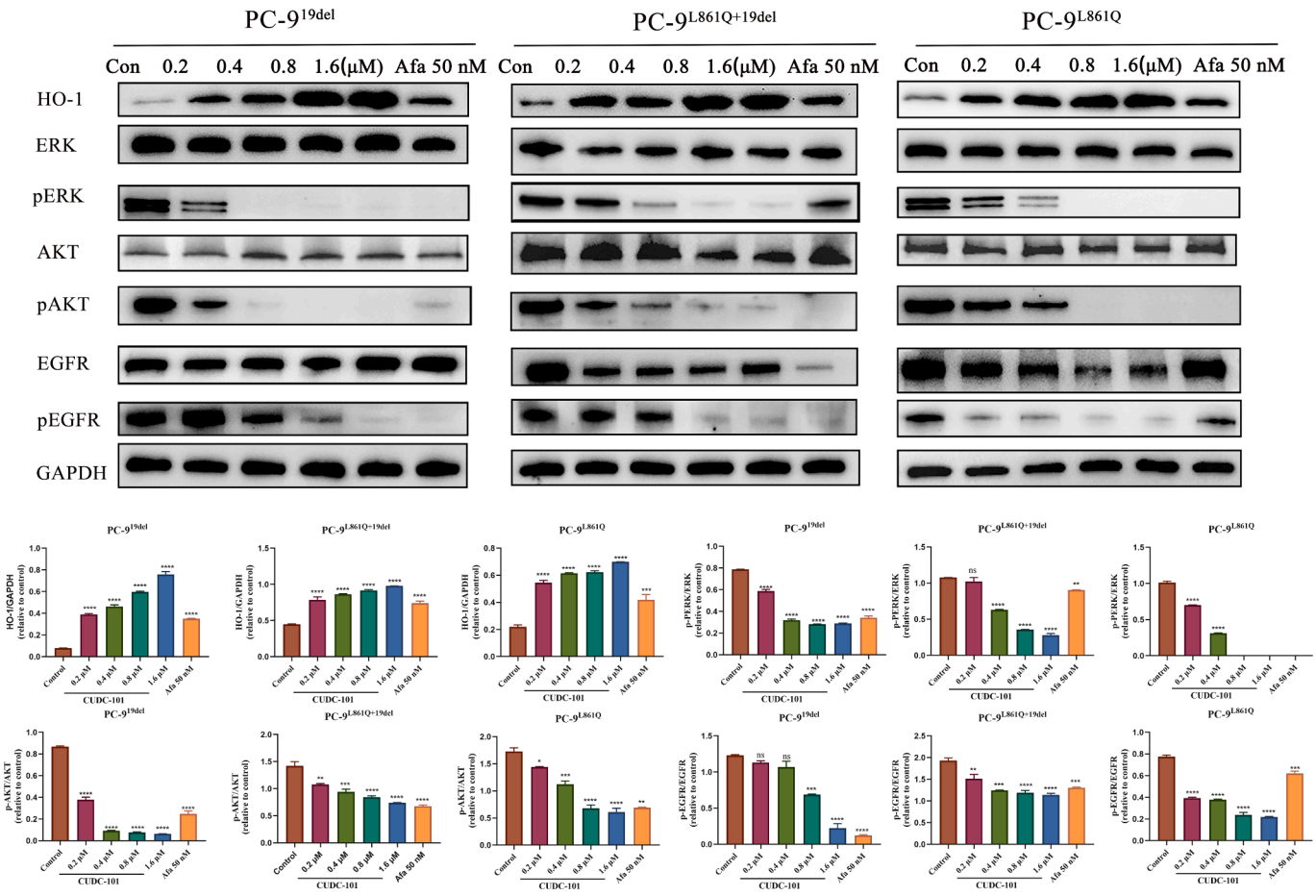

Fig. 8. Effects of CUDC-101 on the expression of relevant proteins in PC9 cell lines. (A) Western blot analysis of the activation of EGFR signalling as indicated by pEGFR, pAKT and pERK levels, and western blot analysis of HO-1 in the three groups cells, PC-9, PC-9$^{L861Q+19del}$ and PC-9^{L861Q} for 48 h with CUDC-101 or afatinib. The ratios of pEGFR/EGFR, pAKT/AKT, pERK/ERK and HO-1/GAPDH were quantified and analysed by Image J software. The data are expressed as a one-way ANOVA for three independent experiments. The results were not statistically significant (ns) or significant at the following levels: $^{*}p < 0.05$, $^{**}p < 0.01$, $^{***}p < 0.001$ and $^{****}p < 0.0001$.

dependent manner, with early and late apoptosis observed in all cell lines (Fig. 5). The percentage of apoptotic cells in the H3255^{L858R} cell line treated by CUDC-101 with 0.2 μM, 0.4 μM, 0.8 μM, 1.6 μM and 50 nM afatinib was 5.88 %, 29.8 %, 35 %, 48.9 %, 60.7 % and 31.5 %, respectively. In contrast, the percentage of apoptotic cells in the H3255$^{L861Q+L858R}$ cell line was 12.05 %, 27.6 %, 30.3 %, 47.6 %, 63.5 % and 26.27 %. In the case of H3255^{L861Q} cells, 12.05 %, 14.95 %, 26.2 %, 27.3 %, 38.4 % and 30.1 %. The percentage in PC-9 cells was 4.95 %, 20.7 %, 38.3 %, 66.4 %, 71.6 % and 34.1 %; in PC-9$^{L861Q+19del}$ cells, 6.33 %, 8.87 %, 13.84 %, 17.21 %, 19.37 % and 8.74 %, respectively; in PC-9^{L861Q} cells, 12.38 %, 28.2 %, 37.8 %, 44.9 %, 48.2 % and 37.8 %, respectively. The results indicated that CUDC-101 exerts an anti-proliferative effect on EGFR L861Q mutant cells by apoptosis.

In order to ascertain the impact of CUDC-101 on the cell cycle of these six cell lines, these cell lines were treated with CUDC-101 (0.2 μM, 0.4 μM, 0.8 μM, 1.6 μM) and 50 nM afatinib, and a PI-FACS assay was then performed 48 h later. CUDC-101 resulted in a significant decrease in S-phase cells and a significant increase in the number of G1-phase cells in H3255, H3255^{L861Q}, H3255$^{L861Q+L858R}$, PC-9, PC-9^{L861Q} and PC-9$^{L861Q+19del}$ cells, indicating that CUDC-101 induced G1-S blocking (Fig. 6).

3.4. Western blot analysis of cells by CUDC-101

In order to investigate the molecular mechanism of cell growth inhibition by CUDC-101, cells were pretreated with different concentrations of CUDC-101 (0.2 μM, 0.4 μM, 0.8 μM, 1.6 μM) and 50 nM afatinib in H3255, H3255^{L861Q}, H3255$^{L861Q+L858R}$, PC-9, PC-9^{L861Q} and PC-9$^{L861Q+19del}$ cells for 48 h, followed by lysis buffer. Given the pivotal role of the ERK and AKT pathways in regulating cell growth based on RNA sequencing, Grey value analysis was conducted using Image J and western blot analysis was employed to assess the expression levels of pEGFR, EGFR, pAKT, AKT, pERK and ERK. The results demonstrated that CUDC-101 inhibited the phosphorylation of EGFR and its downstream signalling substrates AKT and ERK in a dose-dependent manner in these six EGFR mutant cells (Figs. 7 and 8).

Significant differences in sensitivity to EGFR-TKI-induced apoptosis were also observed in afatinib-treated six EGFR mutant cells under different culture conditions. HO-1 is a stress-inducible enzyme that is regarded as an antioxidant and cytoprotective agent. The presence of high levels of HO-1 in tumour cells is typically associated with a reduction in survival (Nitti et al., 2021). The results of the study indicate that CUDC-101 also targets HO-1 and upregulates its expression in six EGFR mutant cell lines (Figs. 7 and 8). In conclusion, these results collectively indicate that CUDC-101 reduces the proliferation of EGFR mutant cells by inducing apoptosis.

4. Discussion

The results of several clinical trials have demonstrated that EGFR-TKI therapy is associated with significantly improved response rates and progression-free survival (PFS) compared to platinum combination

therapy. Consequently, it has been established as the standard of care (Meng et al., 2023). The development of many assays has led to an increase in the detection and identification of EGFR mutations, and this has resulted in the necessity for the development of drugs targeting specific mutations. As the majority of these trials are limited to patients with so-called 'common' EGFR mutations (exon 19 deletion and L858R mutation), there is a paucity of prospective data available to inform treatment decisions for the estimated 7–23 % of EGFR mutation-positive NSCLC tumours carrying rare EGFR mutations, and the objective of this study was to inform treatment decisions for NSCLC tumours (Krawczyk et al., 2017). In the present study, we report on mutational modifications performed on H3255 and PC-9 cells to complete subsequent cytotoxicity assays on EGFR L861Q mutant, respectively.

CUDC-101 is a multi-targeted inhibitor of HDAC, EGFR and HER2, which has demonstrated promising therapeutic effects in the treatment of breast (Zhou et al., 2021), pancreatic (Moertl et al., 2019), and bladder cancers (Wang et al., 2023b). A recent phase I first-in-human trial of CUDC-101 demonstrated that it could be safely administered to patients with solid tumours and effectively induced histone H3 acetylation (Shimizu et al., 2014). These results indicate that CUDC-101 is well tolerated in humans and shows preliminary anti-tumour activity in patients with advanced solid tumours. Studies have demonstrated that different mutations may have different sensitivities to various EGFR TKIs. Currently, few studies have focused on the therapeutic effect of CUDC-101 on the EGFR L861Q mutation in non-small cell lung cancer. Malignant proliferation of tumours represents a significant cause of cancer development and a crucial challenge to be overcome during tumour therapy. The MTT assay and EdU cell proliferation assay experiments demonstrated that CUDC-101 significantly inhibited the growth, viability and proliferation of H3255, H3255^{L861Q}, H3255$^{L861Q+L858R}$, PC-9, PC-9^{L861Q} and PC-9$^{L861Q+19del}$ cells. Subsequent cell cloning experiments provided further confirmation that CUDC-101 exhibited a remarkable inhibitory clonogenic effect in vitro on cells containing NSCLC with EGFR L861Q mutation.

Apoptosis is a process of programmed cell death characterised by chromatin condensation and nuclear fragmentation, accompanied by morphological changes and a reduction in cell volume (Wong, 2011). Preclinical and clinical data indicate that anti-tumour drugs primarily exert their cytotoxic effects by inhibiting cell proliferation and promoting apoptosis. The data obtained from flow cytometry and the observation of cellular mitochondrial membrane potential images demonstrated that CUDC-101 decreased mitochondrial transmembrane potential and induced significant apoptosis in H3255, H3255^{L861Q} and H3255$^{L861Q+L858R}$ cells in a concentration-dependent manner ($p < 0.0001$). A similar effect was observed in PC-9, PC-9^{L861Q} and PC-9$^{L861Q+19del}$ cells, where CUDC-101 decreased the mitochondrial transmembrane potential and triggered significant apoptosis in a concentration-dependent manner.

The cell cycle represents one of the most fundamental processes in cell biology, and abnormal cell proliferation and division are the underlying causes of cancer. The study of the cell cycle helps to elucidate the mechanisms of cancer and other diseases. Our results on the cell cycle assay demonstrated that the cell cycle of H3255, H3255^{L861Q}, H3255$^{L861Q+L858R}$, PC-9, PC-9^{L861Q}, and PC-9$^{L861Q+19del}$ was inhibited by CUDC-101 treatment. The results demonstrated that CUDC-101 treatment resulted in a reduction in the number of cells in the G1 and S phases, accompanied by an increase in the number of cells in the G2/M phase in a dose-dependent manner when compared with the untreated group.

EGFR has been demonstrated that it exhibits high expression activity in numerous solid cancers (Uribe et al., 2021). Our results demonstrated a concentration-dependent decrease in the expression levels of pEGFR, pAKT and pERK in H3255, H3255^{L861Q}, H3255$^{L861Q+L858R}$, PC-9, PC-9^{L861Q} and PC-9$^{L861Q+19del}$ while the expression levels of AKT and ERK remained largely unaltered. The findings indicate that CUDC-101 exerts a pharmacological effect by inhibiting the activation of AKT and ERK signalling pathway. Furthermore, slight differences in the expression of total EGFR were observed in H3255, H3255^{L861Q}, H3255$^{L861Q+L858R}$, PC-9, PC-9^{L861Q}, and PC-9$^{L861Q+19del}$ under the drug treatment. There is also a difference in potency between CUDC-101 and afatanib based on cellular assays, and these differences may be related to the drug targets or caused by other potential reasons, and further investigation is required. In addition, some studies have demonstrated that CUDC-101 regulates the proliferation and migration status of drug-resistant NSCLC HCC827 cells through the down-regulation of the AKT compensation pathway, thereby enabling cancer cells to evade the effects of conventional EGFR/HER-2 inhibitors (Lai et al., 2010). These findings are consistent with those of the present study. HO-1 plays an important role in regulating biological and metabolic processes, as well as in the pathogenesis of a variety of diseases, which has become a topic of significant interest in both domestic and international research (Loboda et al., 2016). The experimental results demonstrated that HO-1 expression was elevated in two common mutant cell lines, H3255 and PC-9, and H3255^{L861Q}, H3255$^{L861Q+L858R}$, PC-9^{L861Q}, and PC-9$^{L861Q+19del}$ cells containing the rare mutant EGFR L861Q mutation following CUDC-101 treatment. All expression levels were increased and this indicates that CUDC-101 may play a beneficial role in preventing oxidative damage and regulating apoptosis. Based on the results of this study, these data support the hypothesis that HDAC combined EGFR inhibition is effective in treating NSCLC, and CUDC-101 is also highly efficacious in a number of other xenograft models and inhibits tumor growth in a dose-dependent manner through interference with multiple pathways and potential synergy (Cai et al., 2010). Our next step in our research program is to refine the validation of the effects of CUDC-101 on more animal studies to eliminate the current limitations due to the lack of xenograft experiments.

Nevertheless, due to the high heterogeneity of uncommon EGFR mutations, further clinical data are required to facilitate the development of personalised therapeutic strategies for individual patients based on specific mutation types. Furthermore, another significant challenge is the detection of uncommon mutations. It is only through the use of appropriate methods and adequate clinical annotation that clinicians can select the most appropriate treatment for each patient.

5. Conclusion

CUDC-101 demonstrated inhibitory effects on cell viability and proliferation, as well as on cell clone formation. It also blocked the cell cycle, decreased the mitochondrial membrane potential, and promoted apoptosis in H3255, H3255^{L861Q}, H3255$^{L861Q+L858R}$, PC-9, PC-9^{L861Q} and PC-9$^{L861Q+19del}$ cells. It can be observed that the aforementioned effects may be achieved by inhibiting the activities of key factors in the ERK and AKT pathways. The results indicate that CUDC-101 has the potential to serve as a targeted therapeutic agent for EGFR L861Q mutation in non-small-cell lung cancer.

CRediT authorship contribution statement

Chunhong Chu: Investigation, Data curation, Validation, Visualization, Writing – original draft. **Huixia Xu:** Methodology, Software. **Chenxue Liu:** Investigation. **Xiangkai Wei:** Investigation. **Lanxin Li:** Investigation, Software. **Rui Wang:** Investigation. **Wenrui Cui:** Methodology. **Guoliang Zhang:** Methodology. **Chenyang Liu:** Methodology. **Ke Wang:** Methodology. **Lei An:** Conceptualization, Resources, Supervision, Project administration, Funding acquisition, Writing – original draft, Writing – review & editing. **Fei He:** Conceptualization, Resources, Supervision, Project administration.

Declaration of competing interest

The authors declare that they have no known competing financial interests or personal relationships that could have appeared to influence

the work reported in this paper.

Data availability

Data will be made available on request.

Acknowledgements

This work was supported by Henan Provincial Science and Technology Research Project (grant number 242102311023); Henan Medical Education Research Project (grant number WJLX2023101); Henan University Teaching Reform Project (grant number HDXJJG2022-146).

Appendix A. Supplementary data

Supplementary data to this article can be found online at https://doi.org/10.1016/j.crtox.2024.100194.

References

An, L., Wang, Y.Q., Wu, G.Y., Wang, Z.X., Shi, Z.Y., Liu, C., Wang, C.L., Yi, M., Niu, C.G., Duan, S.F., Li, X.D., Tang, W.X., Wu, K.M., Chen, S.Q., Xu, H.E., 2023. Defining the sensitivity landscape of EGFR variants to tyrosine kinase inhibitors. Transl. Res. 255, 14–25.

Bae, N.C., Chae, M.H., Lee, M.H., Kim, K.M., Lee, E.B., Kim, C.H., Park, T.I., Han, S.B., Jheon, S., Jung, T.H., Park, J.Y., 2007. and mutations in Korean non-small cell lung cancer patients. Cancer Genet. Cytogenet. 173, 107–113.

Cai, X., Zhai, H.X., Wang, J., Forrester, J., Qu, H., Yin, L., Lai, C.J., Bao, R., Qian, C., 2010. Discovery of 7-(4-(3-ethynylphenylamino)-7-methoxyquinazolin-6-yloxy)-N-hydroxyheptanamide (CUDc-101) as a potent multi-acting HDAC, EGFR, and HER2 inhibitor for the treatment of cancer. J. Med. Chem. 53, 2000–2009.

Evans, M., O'Sullivan, B., Smith, M., Hughes, F., Mullis, T., Trim, N., Taniere, P., 2019. Large-Scale EGFR mutation testing in clinical practice: analysis of a series of 18,920 non-small cell lung cancer cases. Pathol. Oncol. Res. 25, 1401–1409.

Furuyama, K., Harada, T., Iwama, E., Shiraishi, Y., Okamura, K., Ijichi, K., Fujii, A., Ota, K., Wang, S., Li, H.Y., Takayama, K., Giaccone, G., Nakanishi, Y., 2013. Sensitivity and kinase activity of epidermal growth factor receptor (EGFR) exon 19 and others to EGFR-tyrosine kinase inhibitors. Cancer Sci. 104, 584–589.

Gridelli, C., Rossi, A., Carbone, D.P., Guarize, J., Karachaliou, N., Mok, T., Petrella, F., Spaggiari, L., Rosell, R., 2015. Non-small-cell lung cancer. Nat. Rev. Dis. Primers 1.

Ibrahim, T.S., Malebari, A.M., Mohamed, M.F.A., 2021. Design, synthesis, in vitro anticancer evaluation and molecular modelling studies of 3,4,5-trimethoxyphenyl-based derivatives as dual EGFR/HDAC hybrid inhibitors. Pharmaceuticals 14.

Ji, M.Y., Li, Z.L., Lin, Z.H., Chen, L.Y., 2018. Antitumor activity of the novel HDAC inhibitor CUDC-101 combined with gemcitabine in pancreatic cancer. Am. J. Cancer Res. 8, 2402–2418.

Kancha, R.K., Peschel, C., Duyster, J., 2011. The epidermal growth factor receptor-L861Q mutation increases kinase activity without leading to enhanced sensitivity toward epidermal growth factor receptor kinase inhibitors. J. Thorac. Oncol. 6, 387–392.

Kim, Y., Lee, S.H., Ahn, J.S., Ahn, M.J., Park, K., Sun, J.M., 2019. Efficacy and safety of afatinib for mutant non-small cell lung cancer, compared with gefitinib or erlotinib. Cancer Res. Treat. 51, 502–509.

Krawczyk, P., Kowalski, D.M., Ramlau, R., Kalinka-Warzocha, E., Winiarczyk, K., Stencel, K., Powrózek, T., Reszka, K., Wojas-Krawczyk, K., Bryl, M., Wojcik-Superczynska, M., Glogowski, M., Barinow-Wojewódzki, A., Milanowski, J., Krzakowski, M., 2017. Comparison of the effectiveness of erlotinib, gefitinib, and afatinib for treatment of non-small cell lung cancer in patients with common and rare gene mutations. Oncol. Lett. 13, 4433–4444.

Lai, C.J., Bao, R., Tao, X., Wang, J., Atoyan, R., Qu, H., Wang, D.G., Yin, L., Samson, M., Forrester, J., Zifcak, B., Xu, G.X., DellaRocca, S., Zhai, H.X., Cai, X., Munger, W.E., Keegan, M., Pepicelli, C.V., Qian, C.G., 2010. CUDC-101, a multitargeted inhibitor of histone deacetylase, epidermal growth factor receptor, and human epidermal growth factor receptor 2, exerts potent anticancer activity. Cancer Res. 70, 3647–3656.

Liu, C., Wang, Z., Liu, Q., Wu, G., Chu, C., Li, L., An, L., Duan, S., 2022. Sensitivity analysis of EGFR L861Q mutation to six tyrosine kinase inhibitors. Clin. Transl. Oncol. 24, 1975–1985.

Loboda, A., Damulewicz, M., Pyza, E., Jozkowicz, A., Dulak, J., 2016. Role of Nrf2/HO-1 system in development, oxidative stress response and diseases: an evolutionarily conserved mechanism. Cell. Mol. Life Sci. 73, 3221–3247.

Lynch, T.J., Bell, D.W., Sordella, R., Gurubhagavatula, S., Okimoto, R.A., Brannigan, B. W., Harris, P.L., Haserlat, S.M., Supko, J.G., Haluska, F.G., Louis, D.N., Christiani, D. C., Settleman, J., Haber, D.A., 2004. Activating mutations in the epidermal growth factor receptor underlying responsiveness of non-small-cell lung cancer to gefitinib. N. Engl. J. Med. 350, 2129–2139.

Meng, Y., Bai, R.L., Cui, J.W., 2023. Precision targeted therapy for EGFR mutation-positive NSCLC: dilemmas and coping strategies. Thoracic Cancer 14, 1121–1134.

Moertl, S., Payer, S., Kell, R., Winkler, K., Anastasov, N., Atkinson, M.J., 2019. Comparison of radiosensitization by HDAC inhibitors CUDC-101 and SAHA in pancreatic cancer cells. Int. J. Mol. Sci. 20.

Nitti, M., Ivaldo, C., Traverso, N., Furfaro, A.L., 2021. Clinical significance of heme oxygenase 1 in tumor progression. Antioxidants (basel) 10.

Otsuka, T., Mori, M., Yano, Y., Uchida, J., Nishino, K., Kaji, R., Hata, A., Hattori, Y., Urata, Y., Kaneda, T., Tachihara, M., Imamura, F., Katakami, N., Negoro, S., Morita, S., Yokota, S., 2015. Effectiveness of tyrosine kinase inhibitors in Japanese patients with non-small cell lung cancer harboring minor epidermal growth factor receptor mutations: results from a multicenter retrospective study (HANSHIN Oncology Group 0212). Anticancer Res 35, 3885–3891.

Paliogiannis, P., Attene, F., Cossu, A., Defraia, E., Porcu, G., Carta, A., Sotgiu, M.I., Pazzola, A., Cordero, L., Capelli, F., Fadda, G.M., Ortu, S., Sotgiu, G., Palomba, G., Sini, M.C., Palmieri, G., Colombino, M., 2015. Impact of tissue type and content of neoplastic cells of samples on the quality of epidermal growth factor receptor mutation analysis among patients with lung adenocarcinoma. Mol. Med. Rep. 12, 187–191.

Shimizu, T., LoRusso, P.M., Papadopoulos, K.P., Patnaik, A., Beeram, M., Smith, L.S., Rasco, D.W., Mays, T.A., Chambers, G., Ma, A., Wang, J., Laliberte, R., Voi, M., Tolcher, A.W., 2014. Phase I first-in-human study of CUDC-101, a multitargeted inhibitor of HDACs, EGFR, and HER2 in patients with advanced solid tumors. Clin. Cancer Res. 20, 5032–5040.

Sung, H., Ferlay, J., Siegel, R.L., Laversanne, M., Soerjomataram, I., Jemal, A., Bray, F., 2021. Global cancer statistics 2020: GLOBOCAN estimates of incidence and mortality worldwide for 36 cancers in 185 countries. Ca-a Cancer J. Clin. 71, 209–249.

Uribe, M.L., Marrocco, I., Yarden, Y., 2021. EGFR in cancer: signaling mechanisms, drugs, and acquired resistance. Cancers 13.

Wang, Z.X., Li, L.X., Chu, C.H., Wei, X.K., Liu, Q., Wang, R., Zhang, G.L., Wu, G.Y., Wang, Y., An, L., Li, X.D., 2023b. CUDC-101 is a potential target inhibitor for the EGFR-overexpression bladder cancer cells. Int. J. Oncol. 63.

Wang, Y., Liu, Q., Chu, C., Li, L., Wang, Z., Wu, G., Wei, X., An, L., Ma, J., 2023a. Six first-line tyrosine kinase inhibitors reveal novel inhibition potential for the EGFR S768I mutation. Toxicol. Appl. Pharmacol. 461, 116385.

Wong, R.S.Y., 2011. Apoptosis in cancer: from pathogenesis to treatment. J. Exp. Clin. Cancer Res. 30.

Wu, Y.L., Zhou, C.C., Hu, C.P., Feng, J.F., Lu, S., Huang, Y.C., Li, W., Hou, M., Shi, J.H., Lee, K.Y., Xu, C.R., Massey, D., Kim, M., Shi, Y., Geater, S.L., 2014. Afatinib versus cisplatin plus gemcitabine for first-line treatment of Asian patients with advanced non-small-cell lung cancer harbouring EGFR mutations (LUX-Lung 6): an open-label, randomised phase 3 trial. Lancet Oncol. 15, 213–222.

Zappa, C., Mousa, S.A., 2016. Non-small cell lung cancer: current treatment and future advances. Transl. Lung Cancer Res. 5, 288–300.

Zhang, L.S., Zhang, Y.Q., Mehta, A., Boufraqech, M., Davis, S., Wang, J., Tian, Z., Yu, Z. Y., Boxer, M.B., Kiefer, J.A., Copland, J.A., Smallridge, R.C., Li, Z.Y., Shen, M., Kebebew, E., 2015. Dual inhibition of HDAC and EGFR signaling with CUDC-101 induces potent suppression of tumor growth and metastasis in anaplastic thyroid cancer. Oncotarget 6, 9073–9085.

Zhou, Z.L., Van der Jeught, K., Fang, Y.Z., Yu, T., Li, Y.J., Ao, Z., Liu, S., Zhang, L., Yang, Y., Eyvani, H., Cox, M.L., Wang, X.Y., He, X.M., Ji, G., Schneider, B.P., Guo, F., Wan, J., Zhang, X.N., Lu, X.B., 2021. An organoid-based screen for epigenetic inhibitors that stimulate antigen presentation and potentiate T-cell-mediated cytotoxicity. Nat. Biomed. Eng. 5.